Excess quantum noise due to mode nonorthogonality in dielectric microresonators

Henning Schomerus

Department of Physics, Lancaster University, Lancaster, LA1 4YB, United Kingdom

(Dated: June 2009)

This work presents a theory of the frequency-resolved light emission of active two-dimensional dielectric microresonators, which are characterized by a highly non-paraxial mode structure and frequently feature a position-dependent dielectric constant and non-uniform gain. The Lorentzian intensity profile is characterized by an appropriately generalized Petermann factor, a renormalized peak position, and the cold-cavity resonance lifetime Γ. The theory also delivers a relation of Γ to the laser threshold that improves earlier phenomenological expressions even for the case of a homogeneous medium.

Breit-Wigner theory is a cornerstone of the study of open quantum systems and finds numerous applications from atomic and nuclear physics to mesoscopic transport and optical or acoustical resonators. This perturbative theory starts from the isolated situation and delivers a relation between the total scattering cross section and the resonance linewidth $\Delta\omega$. Because of its perturbative nature, Breit-Wigner theory breaks down for moderately open systems. A context which is particularly suited to explore the ensuing new physics are lasers, which are known to emit light around a sharply defined frequency $\bar{\omega}$ with a Lorentzian intensity profile,

$$I(\omega) = \frac{1}{2\pi} \frac{I\Delta\omega}{(\omega - \bar{\omega})^2 + \Delta\omega^2/4}. \tag{1}$$

Here $I = \int d\omega\, I(\omega)$ is the total output intensity. The linewidth is ultimately limited by the spontaneous emission of photons. For almost lossless resonators, the Schawlow-Townes formula relates the quantum-limited linewidth $\Delta\omega_{\rm ST} = \Gamma^2/2I$ to the total output intensity I and the cold-cavity decay rate Γ [1]. This prediction is based on Breit-Wigner theory, and amounts to one spontaneously emitted noise photon per cavity mode. The explicit factor of $1/2$ accounts for the amplitude suppression of field fluctuations due to the active feedback of the medium, and is absent below the lasing threshold.

That the sensitivity to quantum noise increases for more open resonators was first realized by Petermann [2], who considered gain-guided semiconductor lasers. He predicted that the linewidth is enhanced by a factor of $K \geq 1$ such that $\Delta\omega = K\Gamma^2/2I$. Siegman [3] developed a general framework to study open-sided resonators with a paraxial mode structure and arrived at the expression

$$K_0 = \left| \frac{\int |\psi_0|^2 d\mathbf{r}}{\int \psi_0^2 d\mathbf{r}} \right|^2 \tag{2}$$

which relates the Petermann factor to the inverse condition number of the transverse resonance wavefunction ψ_0. This establishes a direct connection to a mathematical measure of mode nonorthogonality. Subsequently, several groups demonstrated the excess noise in experiments on various open-sided resonator geometries with different cross-section [4–8].
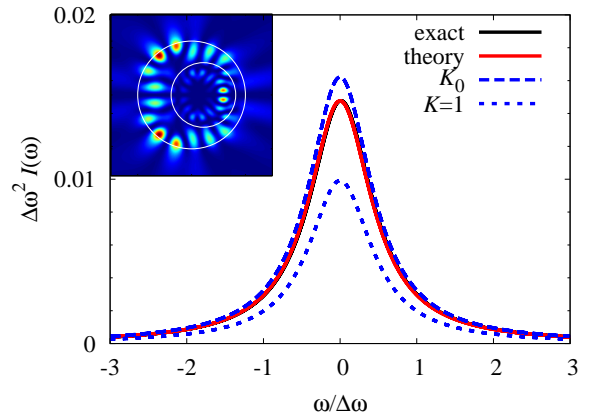

FIG. 1: (Color) Inset: the white circles indicate the dielectric interfaces of an annular resonator with radii $R_2 = 0.6\,R_1$ and eccentricity $d = 0.22\,R_1$. The refractive index in the inner disk is $n_2 = 3.3$, while in the annular region $\operatorname{Re} n_1$ is fixed to 1.8. The color-coded density plot shows a TM-polarized resonator mode at its threshold ($n_{1,0} = 1.8 - i0.029$, $\omega_0 R_1 = 6.45$). Main panel: frequency-resolved intensity close to the threshold (suitably scaled to be independent of the small detuning of $\operatorname{Im} n_1$). The exact numerical result (solid black curve) is a Lorentzian whose width and height can be accurately described using the theory developed in this paper (solid red curve on top of the black curve) [Eq. (3) with parameters determined from Eqs. (4)-(7) (TM polarization)]. A discrepancy in the height is observed when the Petermann factor is determined from the homogeneous expression K_0, Eq. (2) (dashed blue curved), or when it is completely neglected (dotted blue curve, corresponding to the Schawlow-Townes result).

The past decade has seen the development of a new class of microlasers, in which the confinement is due to internal reflection at dielectric interfaces [9–16]. The typical feature size s is often not much larger than the optical wavelength λ. Due to their shape, these resonators support effectively two-dimensional, highly non-uniform, anisotropic modes which are of a decisively non-paraxial character. These systems are currently under intense experimental and theoretical investigations. Until very recently, however, the consequences of mode nonorthogonality have been ignored. Models based on random-

matrix theory [17–20] only partially account for the structured wave patterns of typical microresonators. The first steps into this direction have been taken in recent numerical investigations of stadium billiards [21] and spirals [22], which focus on the case of two cross-talking modes [23] and demonstrate that the Petermann factor can be arbitrarily large even for high-Q modes. Experiments on this subject have just picked up [24]. Therefore, there is a demand for a systematic theory of mode nonorthogonality and its consequences for the quantum noise that accounts for the specific features of dielectric microresonators.

In this paper I fill this gap and develop a theory of the frequency-resolved light emission that applies to general, nonparaxial modes in such resonators and furthermore admits spatial non-uniformity of the dielectric constant and the gain (I assume single mode lasing and therefore also ignore degeneracies of lasing modes). The result entails that formally, the concept of the Petermann factor emerges only in the limit of a small wavelength (or a large resonator), $\lambda/s \ll 1$. In reality, however, the relations given below already work for relatively small resonators (for illustration see Fig. 1, which presents results for an annular microresonator where both the dielectric constant as well as the gain are nonuniform.) The Lorentzian intensity profile can then be parameterized by a few characteristic parameters,

$$I(\omega) = \frac{K}{2\pi} \frac{\Gamma^2 + 4\delta\omega_c^2}{(\omega - \omega_0 - \delta\omega)^2 + \Delta\omega^2/4}. \tag{3}$$

This result contains an appropriately defined Petermann factor in the form of a generalized condition number,

$$K = \left| \frac{\int |\psi_0|^2 \operatorname{Im} n_0^2 \, d\mathbf{r}}{\int \psi_0^2 \operatorname{Im} n_0^2 \, d\mathbf{r}} \right|^2 \quad \text{(TM polarization)}, \tag{4a}$$

$$K = \left| \frac{\int |\nabla\psi_0|^2 \operatorname{Im} n_0^{-2} \, d\mathbf{r}}{\int (\nabla\psi_0)^2 \operatorname{Im} n_0^{-2} \, d\mathbf{r}} \right|^2 \quad \text{(TE polarization)}, \tag{4b}$$

where n_0 is the complex refractive index at threshold, and ψ_0 is the associated resonance wavefunction. The resonance frequency at threshold is denoted by ω_0. Below threshold, the linewidth is given by

$$\Delta\omega = -2 \operatorname{Im} \omega_0 \frac{\int \psi_0^2 n_0 (n_0 - n) \, d\mathbf{r}}{\int \psi_0^2 n_0^2 \, d\mathbf{r}} \quad \text{(TM)}, \tag{5a}$$

$$\Delta\omega = 2 \operatorname{Im} \frac{\int (\nabla\psi_0)^2 n_0^{-3} (n_0 - n) \, d\mathbf{r}}{\omega_0 \int \psi_0^2 \, d\mathbf{r}} \quad \text{(TE)}, \tag{5b}$$

where n is the refractive index at the working point. (Throughout this work the vacuum speed of light $c \equiv 1$; above threshold, the linewidth is further reduced by a factor of $1/2$ [25], as in the Schawlow-Townes case.) The theory also predicts a systematic line shift

$$\delta\omega = \omega_0 \operatorname{Re} \frac{\int \psi_0^2 n_0 (n_0 - n) \, d\mathbf{r}}{\int \psi_0^2 n_0^2 \, d\mathbf{r}} \quad \text{(TM)}, \tag{6a}$$

$$\delta\omega = -\operatorname{Re} \frac{\int (\nabla\psi_0)^2 n_0^{-3} (n_0 - n) \, d\mathbf{r}}{\omega_0 \int \psi_0^2 \, d\mathbf{r}} \quad \text{(TE)}, \tag{6b}$$

which is of the same order as the linewidth and generally only disappears for large resonators filled with a homogeneous medium. The cold-cavity characteristics Γ and $\delta\omega_c$ are obtained from the relation $\delta\omega_c - i\Gamma/2 = \delta\Omega_c$ where

$$\delta\Omega_c = i \frac{\omega_0 \int \psi_0^2 \operatorname{Im} n_0^2 \, d\mathbf{r}}{2 \int \psi_0^2 n_0^2 \, d\mathbf{r}} \quad \text{(TM)}, \tag{7a}$$

$$\delta\Omega_c = -i \frac{\int (\nabla\psi_0)^2 \operatorname{Im} n_0^{-2} \, d\mathbf{r}}{2\omega_0 \int \psi_0^2 \, d\mathbf{r}} \quad \text{(TE)}. \tag{7b}$$

As a notable side product, the latter expressions generalize and improve the common phenomenological relation $\operatorname{Im} n_0 = -(2\Gamma/\omega_0) \operatorname{Re} n_0$ (TM) between the cold-cavity lifetime and the laser threshold of homogenous systems.

All considerations in this paper are based on the effective-medium approach, where the geometric and material-specific properties of a dielectric microresonator are described by a position-dependent refractive index $n(\mathbf{r})$. Let us assume $n(\mathbf{r}) = 1$ outside the resonator. Inside the resonator the refractive index can be complex, with $\operatorname{Im} n < 0$ in the amplifying (active) regions of the medium. For an effectively two-dimensional resonator, the classical electromagnetic field is represented by a scalar wavefunction $\psi(\mathbf{r}; \omega)$ which fulfills the Helmholtz equation [26]

$$\mathcal{L}\psi(\mathbf{r}; \omega) = 0, \quad \mathcal{L} = \Delta + \omega^2 n^2(\mathbf{r}) \quad \text{(TM)}, \tag{8a}$$

$$\mathcal{L} = \nabla n^{-2}(\mathbf{r})\nabla + \omega^2 \quad \text{(TE)}. \tag{8b}$$

Consider the case that $\operatorname{Re} n(\mathbf{r})$ is fixed while $\operatorname{Im} n(\mathbf{r})$ can be controlled via pumping. At the laser threshold $\operatorname{Im} n(\mathbf{r}) \equiv \operatorname{Im} n_0(\mathbf{r})$, Eq. (8) admits a solution ψ_0 satisfying purely outgoing boundary conditions with real angular frequency ω_0. Below the laser threshold, the resonance frequency Ω associated to this solution becomes complex, where $-2 \operatorname{Im} \Omega = \gamma$ is the decay rate. The cold-cavity decay rate Γ is obtained for $\operatorname{Im} n = 0$ (the complex cold-cavity resonance frequency is denoted by $\Omega_c = \omega_c - i\Gamma/2$).

Quantum optics adds spontaneously emitted photons to this picture, which are generated and amplified by the active medium. Even in absence of external illumination, the resonator then emits photons of frequency $\omega \approx \operatorname{Re} \Omega$. A convenient quantum-optical framework to study this radiation is provided by the input-output formalism, which delivers the output intensity [19, 27]

$$I(\omega) = \frac{1}{2\pi} \operatorname{tr} (S^\dagger S - \mathbb{1}) \tag{9}$$

in terms of the scattering matrix $S(\omega)$ of the classical field (assuming complete population inversion in the medium).

For the cold cavity the scattering matrix is unitary, and the passive resonator does not emit any radiation. For a finite gain the scattering matrix departs from unitarity because the particle flux is no longer conserved due to the stimulated emission of photons in the active medium. Even if the cold-cavity resonances are strongly overlapping for the cold cavity (as is typical for low-Q modes

with Γ larger than the mode spacing), well-resolved resonances appear when one steers the system close to the laser threshold. Dielectric microresonator design aims to support high-Q modes, which can be resolved even deep below threshold [21, 24]; in that case, however, the threshold is reached more quickly than in the case of low-Q modes. Both cases can therefore be approached by a systematic expansion around the threshold condition [28], which delivers the output intensity

$$I(\omega) = \frac{1}{2\pi} \left| \frac{\int |\psi_0|^2 \, \mathrm{Im}\, n_0^2 \, d\mathbf{r}}{\int \psi_0^2 n_0^2 (\omega/\omega_0 + n/n_0 - 2)\, d\mathbf{r}} \right|^2 \quad \text{(TM)}, \quad (10\mathrm{a})$$

$$I(\omega) = \frac{1}{2\pi} \left| \frac{\int |\nabla\psi_0|^2 \, \mathrm{Im}\, n_0^{-2} \, d\mathbf{r}}{\omega_0(\omega - \omega_0)\int \psi_0^2 \, d\mathbf{r} + \int (\nabla\psi_0)^2 \frac{n-n_0}{n_0^3}\, d\mathbf{r}} \right|^2 \quad \text{(TE)}. \tag{10b}$$

This expression formally diverges at the complex frequency $\Omega = \omega_0 + \delta\Omega$ where

$$\delta\Omega = \omega_0 \frac{\int \psi_0^2 n_0 (n_0 - n)\, d\mathbf{r}}{\int \psi_0^2 n_0^2 \, d\mathbf{r}} \quad \text{(TM)}, \tag{11a}$$

$$\delta\Omega = -\frac{\int (\nabla\psi_0)^2 n_0^{-3}(n_0 - n)\, d\mathbf{r}}{\omega_0 \int \psi_0^2 \, d\mathbf{r}} \quad \text{(TE)}, \tag{11b}$$

The output intensity is hence a Lorentzian [Eq. (1)] whose center $\bar{\omega} = \mathrm{Re}\,\Omega$ is displaced from ω_0 by a systematic line shift $\delta\omega = \mathrm{Re}\,\delta\Omega$ [see Eq. (6)], which is generally of the same order as the width $\Delta\omega = -2\,\mathrm{Im}\,\delta\Omega$ of the Lorentzian [see Eq. (5)]. The latter can be related to the total intensity $I = \int I(\omega)\, d\omega$ via the relation

$$\Delta\omega = \frac{1}{I} \left| \frac{\omega_0 \int |\psi_0|^2 \, \mathrm{Im}\, n_0^2 \, d\mathbf{r}}{\int \psi_0^2 n_0^2 \, d\mathbf{r}} \right|^2 \quad \text{(TM)}, \tag{12a}$$

$$\Delta\omega = \frac{1}{I} \left| \frac{\int |\nabla\psi_0|^2 \, \mathrm{Im}\, n_0^{-2} \, d\mathbf{r}}{\omega_0 \int \psi_0^2 \, d\mathbf{r}} \right|^2 \quad \text{(TE)}. \tag{12b}$$

This expression contains integrals similar to those in the expression for K_0 [Eq. (2)], but weighted by the refractive index. Moreover, instead of the transverse mode profile, ψ_0 now represents the resonance wavefunction in the resonator plane, which encodes the full, non-paraxial mode structure. At this point, the integral in the denominator is not restricted to the interior of the resonator, and the result does not feature the cold-cavity decay rate. For the latter reason Eq. (12) cannot be used to extract a generalized Petermann factor.

In order to make contact with the conventional theory of the linewidth we now consider the regime $\lambda \ll s$ of a large resonator. Under this condition, typical resonances have a small cold-cavity decay rate, $\Gamma \ll \omega_0$, and the laser threshold is attained at a small gain, $|\mathrm{Im}\, n_0| \ll \mathrm{Re}\, n_0$. Equation (11) then applies all the way down to the cold-cavity limit, and can be further recast to deliver the complex cold-cavity resonance frequency $\Omega_c = \omega_0 + \delta\Omega_c$, where $\delta\Omega_c$ is given by Eq. (7). This result is perturbative in the gain but nonperturbative in the openness of the system, which is encoded in ω_0, n_0, and ψ_0. Note that in Eq. (7), the numerator is determined by the active region, while the denominator also depends on the passive regions — including the region outside the resonator, where integrals are well defined because n is real [29]. For homogeneous systems, the simple relation $\Omega_c = \omega_0 + i(\mathrm{Im}\, n_0/\mathrm{Re}\, n_0)\omega_0$ (TM) is often applied (this also entails the relation for the laser threshold discussed above). In comparison to Eq. (7), this simple expression is only valid when one can ignore to the exterior contribution to the denominator, which in practice requires a very large system size.

With Eq. (7), linewidth (12) simplifies to

$$\Delta\omega = \frac{\Gamma^2 + 4\delta\omega_c^2}{I} \left| \frac{\int |\psi_0|^2 \, \mathrm{Im}\, n_0^2 \, d\mathbf{r}}{\int \psi_0^2 \, \mathrm{Im}\, n_0^2 \, d\mathbf{r}} \right|^2 \quad \text{(TM)}, \tag{13a}$$

$$\Delta\omega = \frac{\Gamma^2 + 4\delta\omega_c^2}{I} \left| \frac{\int |\nabla\psi_0|^2 \, \mathrm{Im}\, n_0^{-2} \, d\mathbf{r}}{\int (\nabla\psi_0)^2 \, \mathrm{Im}\, n_0^{-2} \, d\mathbf{r}} \right|^2 \quad \text{(TE)}, \tag{13b}$$

which features the cold-cavity decay rate $\Gamma = -2\,\mathrm{Im}\,\delta\Omega_c$ along with the cold-cavity line shift $\delta\omega_c = \mathrm{Re}\,\delta\Omega_c$. (Far above the laser threshold, the linewidth is again halved because amplitude fluctuations are suppressed by the nonlinear feedback with the medium [25]). The Petermann factor, hence, takes the form of Eq. (4). For TM polarization, the conventional form [Eq. (2)] of the Petermann factor is recovered when the active medium fills the resonator homogeneously (so that n_0 does not depend on position). This conceptual relation hence applies even when the mode structure in the resonator plane is strongly non-paraxial. This is also the case for TE polarization or an inhomogeneous medium, where Eq. (4) relates the excess noise to an appropriately generalized measure of mode nonorthogonality (satisfying $K \to 1$ in the limit of a closed resonator). For an inhomogeneous medium, Eq. (4) shows that the excess noise is generated in the active regions (where $\mathrm{Im}\, n_0 \neq 0$).

Model system. In order to assess the predictive power of the above analysis I turn to a paradigmatic example of a microresonator with a nonuniform refractive index, which at the same time displays a rich variety of resonator modes. This is provided by the annular microresonator geometry, defined by two eccentric circular interfaces such as indicated in the inset of Fig. 1. In order to exploit the full generality of the formalism presented above, I assume that the gain is constrained to the annular region between these interfaces ($\mathrm{Im}\, n_1 \equiv -i\tilde{n}$), but vanishes in the interior disk ($\mathrm{Im}\, n_2 = 0$), and furthermore set $\mathrm{Re}\, n_1 = 1.8$ and $\mathrm{Re}\, n_2 = 3.3$. The radii of the two circles are related by $R_2 = 0.6\, R_1$, and the eccentricity is $d = 0.22\, R_1$. The finite eccentricity breaks the rotational symmetry and hence leads to nonintegrable classical ray dynamics. The classical phase space accommodates domains of stability embedded into regions of chaotic instability and, hence, exhibits the full complexity of generic dynamical systems. The corresponding wave dynamics reflect this complexity in a rich set of resonance wavefunctions, which also includes examples with

a highly directional far-field radiation pattern [30, 31].

Numerical techniques make it possible to investigate a large number of modes, especially in the interesting regime where $\omega_0 R_1$ is moderately large [30]. Here I focus on a representative example of a resonator mode with TM polarization, which reaches its threshold at $\tilde{n}_0 = 0.029$, $\omega_0 R_1 = 6.45$. In the main panel of Fig. 1, the solid black curve shows the intensity profile close to threshold (for a small detuning of $\tilde{n}$), which is directly obtained from Eq. (9) via a numerical computation of the scattering matrix. The curve is scaled so that it becomes independent of the detuning when $\tilde{n} - \tilde{n}_0$ is small. The red curve is obtained from the theory developed in this work: a Lorentzian of form (3), where the parameters are determined by Eqs. (4)-(7) (for TM polarization). This curve lies on top of the black curve so that the latter is barely visible. The theory of this paper hence applies even though the resonator is only moderately larger than the wavelength. The other curves illustrate the necessity to adopt the results developed in this paper. The dashed blue curve is obtained when the Petermann factor is taken of the homogeneous form K_0 [Eq. (2)], while the dotted blue curve shows the result when mode nonorthogonality is entirely ignored (as in Breit-Wigner theory, which delivers the Shawlow-Townes formula) [32].

For completeness I remark that in the case of a homogeneous circular disk resonator (corresponding to $R_2 = 0$), Eq. (2) applies. In polar coordinates, the radial dependence is given by Bessel functions, while the constraint on time-reversal symmetry singles out modes with a standing-wave angular dependence $\sin(m(\phi - \phi_0))$ [30]. For TM polarization and $\omega R \gg 1$, Petermann factor (2) then takes the asymptotic form $K = \sinh^2 x / x^2$ where $x = 2\,\mathrm{Im}\,(n\omega R_1)$ and therefore approaches unity for modes with a large Q factor.

In summary, I have explored the consequences of mode nonorthogonality in dielectric microresonators for the general case of a highly non-paraxial mode structure and nonuniform material properties. This theory leads to an appropriately generalized Petermann factor [Eq. (4)]. Compact expressions (3)-(7) can be used to inform the interpretation of experiments beyond the simple effective phenomenological models employed to date. An open question (beyond the illustrative example of Fig. 1) that can be pursued on basis of these expressions is how complex quantum dynamics (regular versus chaotic wave patterns) express themselves in the mode nonorthogonality.

[1] A. L. Schawlow and C. H. Townes, Phys. Rev. **112**, 1940 (1958).
[2] K. Petermann, IEEE J. Quantum Electron. **15**, 566 (1979).
[3] A. E. Siegman, Phys. Rev. A **39**, 1253 (1989).
[4] W. A. Hamel and J. P. Woerdman, Phys. Rev. Lett. **64**, 1506 (1990).
[5] Y.-J. Cheng, C. G. Fanning, and A. E. Siegman, Phys. Rev. Lett. **77**, 627 (1996).
[6] M. A. van Eijkelenborg, Å. M. Lindberg, M. S. Thijssen, and J. P. Woerdman, Phys. Rev. Lett. **77**, 4314 (1996).
[7] M. A. van Eijkelenborg, Å. M. Lindberg, M. S. Thijssen, and J. P. Woerdman, Phys. Rev. A **55**, 4556 (1997).
[8] A. M. van der Lee, N. J. van Druten, A. L. Mieremet, M. A. van Eijkelenborg, Å. M. Lindberg, M. P. van Exter, and J. P. Woerdman, Phys. Rev. Lett. **79**, 4357 (1997).
[9] C. Gmachl, F. Capasso, E. E. Narimanov, J. U. Nöckel, A. D. Stone, G. J. Faist, D. L. Sivco, and A. Y. Cho, Science **280**, 1556 (1998).
[10] N. B. Rex, H. E. Tureci, H. G. L. Schwefel, R. K. Chang, and A. D. Stone, Phys. Rev. Lett. **88**, 094102 (2002).
[11] S.-B. Lee, J.-H. Lee, J.-S. Chang, H.-J. Moon, S. W. Kim, and K. An, Phys. Rev. Lett. **88**, 033903 (2002).
[12] T. Harayama, T. Fukushima, S. Sunada, and K. S. Ikeda, Phys. Rev. Lett. **91**, 073903 (2003).
[13] M. Lebental, J. S. Lauret, R. Hierle, and J. Zyss, Appl. Phys. Lett. **88**, 031108 (2006).
[14] T. Fukushima and T. Harayama, IEEE J. Sel. Top. Quantum Electron. **10**, 1039 (2004).
[15] T. Fukushima, T. Harayama, and J. Wiersig, Phys. Rev. A **73**, 023816 (2006).
[16] S.-Y. Lee, S. Rim, J.-W. Ryu, T.-Y. Kwon, M. Choi, and C.-M. Kim, Phys. Rev. Lett. **93**, 164102 (2004).
[17] M. Patra, H. Schomerus, and C. W. J. Beenakker, Phys. Rev. A **61**, 023810 (2000).
[18] K. Frahm, H. Schomerus, M. Patra, and C. W. J. Beenakker, Europhys. Lett. **49**, 48 (2000).
[19] H. Schomerus, K. Frahm, M. Patra, and C. W. J. Beenakker, Physica A **278**, 469 (2000).
[20] J. P. Keating, M. Novaes, and H. Schomerus, Phys. Rev. A **77**, 013834 (2008).
[21] S.-Y. Lee, J.-W. Ryu, J.-B. Shim, S.-B. Lee, S. W. Kim, and K. An, Phys. Rev. A **78**, 015805 (2008).
[22] J. Wiersig, S. W. Kim, and M. Hentschel, Phys. Rev. A **78**, 053809 (2008).
[23] M. V. Berry, J. Mod. Opt. **50**, 63 (2003)
[24] S.-B. Lee *et al.*, arXiv:0904.0416; arXiv:0905.4478.
[25] P. Goldberg, P. W. Milonni, and B. Sundaram, Phys. Rev. A **44**, 1969 (1991).
[26] C. Vassallo, *Optical Waveguide Concepts* (Elesvier, Amsterdam, 1991).
[27] C. W. J. Beenakker, Phys. Rev. Lett. **81**, 1829 (1998).
[28] See Appendix A for details of the derivation.
[29] For a practical method to reduce the integration to a finite domain, draw a circle of radius R around the resonator and use $\int_R^\infty r H_n^{(+)\,2}(\omega r)\, dr = -\frac{1}{2} R^2 [H_n^{(+)\,2}(\omega R) - H_{n+1}^{(+)}(\omega R) H_{n-1}^{(+)}(\omega R)]$ in the basis of Hankel functions.
[30] M. Hentschel and K. Richter, Phys. Rev. E **66**, 056207 (2002).
[31] J. Wiersig and M. Hentschel, Phys. Rev. A **73**, 031802(R) (2006).
[32] For further modes see Appendix B.

APPENDIX A: FURTHER DETAILS OF THE DERIVATION

This appendix details some technical steps in the derivation of Eq. (10). The analysis exploits that near resonance, the outgoing radiation is dominated by the resonance wavefunctions, $\psi \approx \psi_0$. To be specific, let us consider a disk $\mathcal{C}$ of radius $R \to \infty$ that completely covers the resonator, so that outside the disk $n(\mathbf{r}) = 1$. Using polar coordinates r, φ in a coordinate system with origin at the center of the disk, a basis of scattering wavefunctions is then given by

$$\phi_m^{(\sigma)}(r, \varphi; \omega) = H_m^{(\sigma)}(\omega r) e^{i\sigma m \varphi}, \tag{A1}$$

where H is the Hankel function and $m = 0, \pm 1, \pm 2, \ldots$. The index σ takes the value $\sigma = +$ for outgoing scattering states while $\sigma = -$ for incoming scattering states.

The expansion of the scattering wavefunction in the basis (A1) defines, respectively, the in- and outgoing scattering amplitudes a_m and b_m,

$$\psi(\mathbf{r}) = \sum_m \left[b_m \phi_m^{(+)}(r, \varphi) + a_m \phi_m^{(-)}(r, \varphi) \right]. \tag{A2}$$

Adopting a vector notation the amplitudes are related via the scattering matrix S, $\mathbf{b} = S\mathbf{a}$, which is found by matching the scattering states to solutions of Eq. (8a) inside the disk. The expansion coefficients of the resonance wavefunction in the scattering region are denoted by $\mathbf{b}_0$.

The following considerations rest on a consequence of the divergence theorem,

$$\int_{\mathcal{C}} d\mathbf{r}\, \psi_1 \Delta \psi_2 = \int_{\mathcal{C}} d\mathbf{r}\, \psi_2 \Delta \psi_1 + \oint_{\partial \mathcal{C}} d\varphi\, R \left[\psi_1 \frac{\partial \psi_2}{\partial r} - \psi_2 \frac{\partial \psi_1}{\partial r} \right], \tag{A3}$$

which holds for arbitrary well-behaved functions ψ_1, ψ_2, and the orthogonality property

$$\oint_{\partial \mathcal{C}} d\varphi\, R \left[\phi_m^{(\sigma)} \frac{\partial \phi_{m'}^{(\sigma')}}{\partial r} - \phi_{m'}^{(\sigma')} \frac{\partial \phi_m^{(\sigma)}}{\partial r} \right] = 4i(\sigma' - \sigma)\delta_{m,m'} \tag{A4}$$

of the scattering basis functions (∂C denotes the circular boundary of the disk $\mathcal{C}$, which eventually moves to infinity).

Due to time-reversal symmetry, the scattering matrix is symmetric, $S = S^T$. To see that this symmetry holds for complex n, consider two arbitrary solutions ψ_1, ψ_2 of the Helmholtz equation, and apply the definition of the scattering matrix as well as Eqs. (A3) and (A4) to evaluate

$$-8i\mathbf{a}_2^T(S - S^T)\mathbf{a}_1 = \int_{\mathcal{C}} (\psi_2 \mathcal{L} \psi_1 - \psi_1 \mathcal{L} \psi_2)\, d\mathbf{r} = 0. \tag{A5}$$

Close the resonance, the outgoing radiation will be dominated by the characteristics of the resonant state. Hence, $S \approx \alpha \mathbf{b}_0 \mathbf{b}_0^T$, where α diverges at the resonance so that other outgoing wave components can be ignored.

The evaluation of the coefficient α requires to compute the overlap between the resonance wavefunction ψ_0 and an arbitrary near-resonant solution $\psi \approx \psi_0$, which also possesses a small incoming component. Assume that ψ is normalized so that the dominant outgoing radiation is described by the amplitudes $\mathbf{b}_0$. The scattering matrix then takes the form $S \approx \mathbf{b}_0 \mathbf{b}_0^T / (\mathbf{b}_0^T \mathbf{a})$, while the intensity becomes

$$I \approx \frac{1}{2\pi} \frac{|\mathbf{b}_0^\dagger \mathbf{b}_0|^2}{|\mathbf{b}_0^T \mathbf{a}|^2}. \tag{A6}$$

In both expressions the denominator is independent of the choice of the near-resonant wavefunction ψ:

$$-8i\mathbf{b}_0^T \mathbf{a} = \int [\psi_0(\Delta \psi) - \psi(\Delta \psi_0)]\, d\mathbf{r}$$
$$\approx \int \psi_0^2 (n^2 \omega^2 - n_0^2 \omega_0^2)\, d\mathbf{r}, \tag{A7}$$

where in the last step we used the Helmholtz equation. As we are close to resonance, $n^2 \omega^2 - n_0^2 \omega_0^2 \approx 2n_0^2 \omega_0^2(\omega/\omega_0 + n/n_0 - 2)$.

We now once more exploit time-reversal symmetry, this time in the form that ψ_0^* provides a purely incoming solution of the Helmholtz equation where $n_0 \to n_0^*$. Therefore,

$$-8i\mathbf{b}_0^\dagger \mathbf{b}_0 = \int [\psi_0(\Delta \psi_0^*) - \psi_0^*(\Delta \psi_0)]\, d\mathbf{r}$$
$$= \int |\psi_0|^2 (n_0^2 - n_0^{*2})\omega_0^2\, d\mathbf{r}. \tag{A8}$$

Equation (10a) now follows from Eqs. (A6), (A7), and (A8). The techniques described above can also be adapted to modes with TE polarization which are governed by the Helmholtz equation (8b); this then results in Eq. (10b).
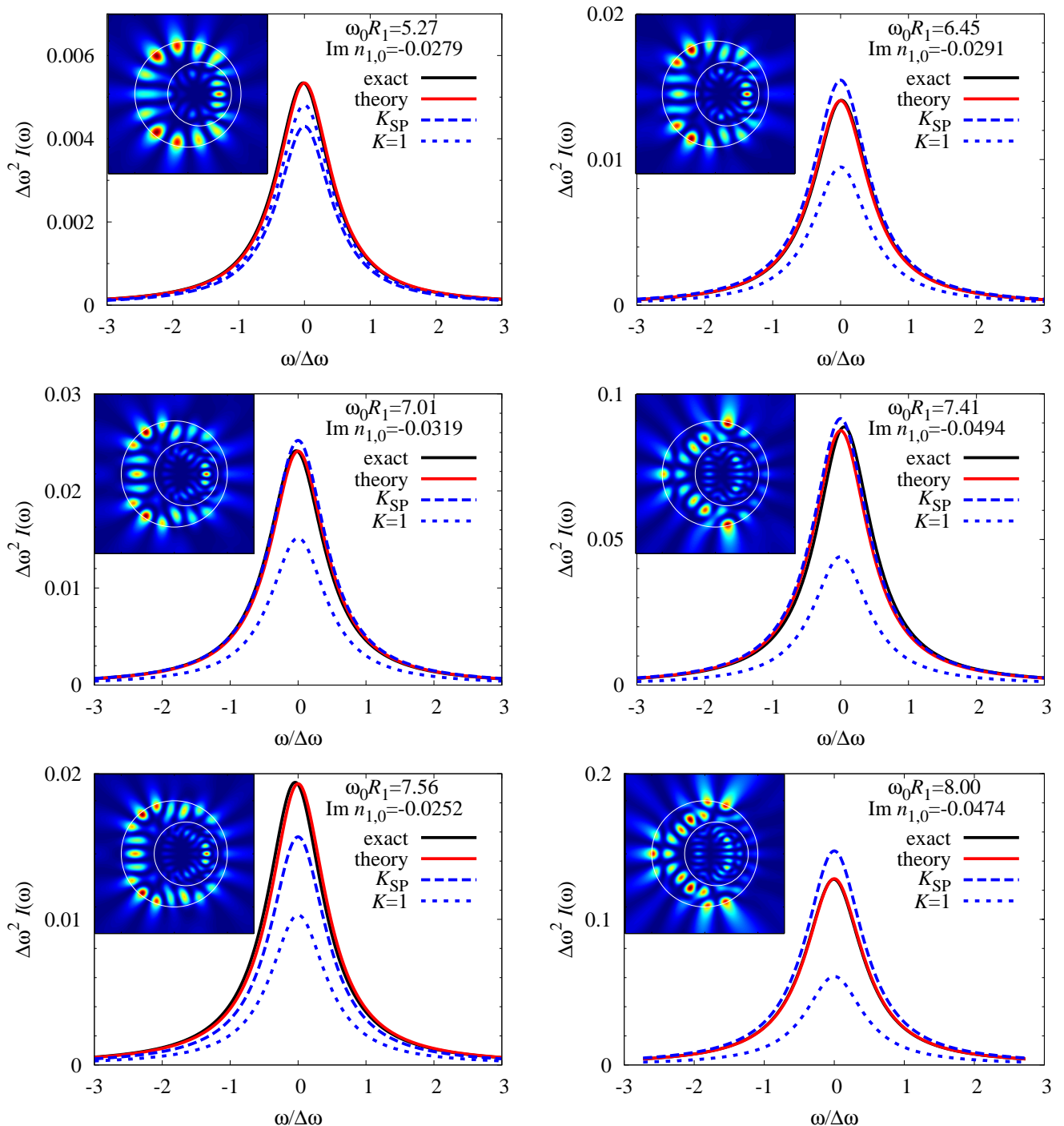
APPENDIX B: COMPARISON TO OTHER RESONATOR MODES

FIG. 2: (Color) Same as Fig. 1, but for other resonator modes of the annular resonator. All modes have even parity with respect to the horizontal resonator axis. The mode with $\omega_0 R_1 = 6.45$ is almost degenerate with the odd-parity mode of Fig. 1.